



Published in final edited form as:

Invest Radiol. 2009 June ; 44(6): 343–350. doi:10.1097/RLI.0b013e3181a64ce9.

Predicting Control of Primary Tumor and Survival by DCE MRI During Early Therapy in Cervical Cancer

William T.C. Yuh, MD, MSEE¹, Nina A. Mayr, MD², David Jarjoura, PhD³, Dee Wu, PhD², John C. Grecula, MD², Simon S. Lo, MD², Susan M. Edwards, MD⁴, Vincent A. Magnotta, PhD⁵, Steffen Sammet, MD, PhD¹, Hualin Zhang, PhD², Joseph F. Montebello, MD², Jeffrey Fowler, MD², Michael V. Knopp, MD, PhD¹, and Jian Z. Wang, PhD²

¹ Department of Radiology, Ohio State University, Columbus, Ohio, USA

² Department of Radiation Medicine, Ohio State University, Columbus, Ohio, USA

³ Center for Biostatistics, Ohio State University, Columbus, Ohio, USA

⁴ Department of Radiological Sciences, University of Oklahoma Health Sciences Center, Oklahoma City, Oklahoma, USA

⁵ Department of Radiology, University of Iowa, Iowa City, IA, USA

Abstract

Purpose—To assess the early predictive power of MRI perfusion and volume parameters, during early treatment of cervical cancer, for primary tumor control and disease-free-survival.

Materials and Methods—Three MRI examinations were obtained in 101 patients before and during therapy (at 2–2.5 and 4–5 weeks) for serial dynamic contrast enhanced (DCE) perfusion MRI and 3-dimensional (3D) tumor volume measurement. Plateau Signal Intensity (SI) of the DCE curves for each tumor pixel of all 3 MRI examinations was generated, and pixel-SI distribution histograms were established to characterize the heterogeneous tumor. The degree and quantity of the poorly-perfused tumor subregions, which were represented by low-DCE pixels, was analyzed by using various lower percentiles of SI (SI%) from the pixel histogram. SI% ranged from SI2.5% to SI20% with increments of 2.5%. SI%, mean SI, and 3D-volume of the tumor were correlated with primary tumor control and disease-free-survival, using Student *t*-test, Kaplan-Meier analysis and log-rank test. The mean post-therapy follow-up time for outcome assessment was 6.8 years (range: 1.2–12.3 years).

Results—Tumor volume, mean SI, and SI% showed significant prediction of the long-term clinical outcome, and this prediction was provided as early as 2–2.5 weeks into treatment. An SI5% of <2.05 and residual tumor volume of ≥ 30 cm³ in the MRI obtained at 2–2.5 weeks of therapy provided the best prediction of unfavorable 8-year primary tumor control (73% vs. 100%, *p*=0.006) and disease-free-survival rate (47% vs. 79%, *p*=0.001), respectively.

Conclusions—Our results show that MRI parameters quantifying perfusion status and residual tumor volume provide very early prediction of primary tumor control and disease-free-survival. This functional imaging based outcome predictor can be obtained in the very early phase of cytotoxic therapy within 2–2.5 weeks of therapy start. The predictive capacity of these MRI parameters, indirectly reflecting the heterogeneous delivery pattern of cytotoxic agents, tumor oxygenation and the bulk of residual presumably therapy-resistant tumor, requires future study.

Keywords

MRI; Functional; Microcirculation; Uterine cervical neoplasms; Radiotherapy

Introduction

Advanced cervical cancer is a disease, where early prediction of therapy outcome is of paramount importance. Once the therapy failure is detected many months or years after the completion of first-line treatment, the salvage treatment options are exceedingly poor.¹ The information from post-therapy imaging after treatment completion, which is commonly employed for response assessment, usually comes too late to realistically impact patient management. Conversely, if therapy failure can be predicted effectively and as early as possible in the initial course of treatment, clinical management can be profoundly impacted in the individual patient.

Such early outcome prediction has been challenging in cervical cancer, and the prognosis of the disease is known to vary greatly within stage and currently used prognostic categories.² A critical clinical challenge has been the lack of non-invasive and clinically validated means to predict the long-term treatment outcome specific to a therapeutic regimen early during the treatment course, when the morphological and physiological changes of the tumor are subtle. Early prediction of treatment failure in those patients, in whom the ongoing therapy regimen will ultimately not be successful, can provide a window of opportunity to change the initial therapy approach *upfront* - instead of *after* the tumor has already recurred. Because the salvage therapy options are so poor once the tumor has recurred, the prediction of therapy failure must occur sufficiently early, within the first few weeks of the *initial* treatment course to realistically impact outcome. At this early time point, more aggressive treatment regimens, including radiation dose intensification, changes in concurrent chemotherapy and/or novel experimental clinical trial treatments, can be implemented *in time and upfront* for those patients, who are at high risk to fail ongoing conventional therapy.

Functional/biological tumor properties, including vascularity and hypoxia, provide a new opportunity to develop predictors of therapy success. Novel imaging methods are being explored to assess tumor vascularity³⁻¹¹. Vascular characteristics and hypoxia of tumors are known to profoundly influence tumor responsiveness and treatment outcome to cytotoxic therapy, including radiation and chemotherapy.¹²⁻¹⁵ Dynamic contrast-enhanced (DCE) MRI has shown promise in assessing tumor vascularity, perfusion and indirectly tumor hypoxia during cytotoxic therapy,^{3-6,16,17} and correlations of DCE MRI with therapy outcome have been suggested.^{4,6,16-19}

The optimal DCE MRI and tumor volume parameters and the best timing of the imaging in clinical patients with respect to the treatment course have not been conclusively established. To translate the DCE MRI from the experimental stage into clinical practice, the validation of the DCE MRI imaging parameters is needed through treatment outcome correlation in sufficiently large patient series with systematic and solid long-term post-therapy follow-up.

The purpose of this study was to assess the early predictive power of MRI perfusion and volume parameters, during early treatment of cervical cancer, for primary tumor control and disease-free-survival, based upon the heterogeneous tumor perfusion status using DCE MRI and MRI-based 3-dimensional (3D) tumor volume measurement derived from three sequential MRI examinations obtained prospectively before and during cytotoxic therapy in cervical cancer. The study sought to identify the type and timing of the imaging parameters with the best prediction of outcome.

Materials and Methods

Patients and Selection Criteria

One-hundred-and-one patients with biopsy-proven advanced cervical cancer, who were treated with radiation and chemotherapy, were prospectively studied on an IRB approved imaging protocol. Patients with stages IB₂-IVA squamous cell, adenocarcinoma or adenosquamous carcinoma, but not small cell neuroendocrine carcinoma were included. Three sequential MRI examinations were performed: before treatment (MRI 1), at 2–2.5 weeks (MRI 2) and at 4–5 weeks (MRI 3) into the 8-week radiation therapy course. Standard-of-care radiation therapy was delivered using a dose of 45–50 Gy in 1.8–2.0 Gy fractions of external beam radiation therapy, that was integrated with standard brachytherapy (dose 14–61 Gy, mean: 40.4 Gy), starting after MRI 3 in all but 9 patients. The treatment regimen was not altered based on any MR imaging findings of this ongoing research.

Pre- and Post-contrast MRI

All patients were studied with 1.5 Tesla MR scanners (GE Medical Systems, Milwaukee, WI; Somatom, Siemens, Erlangen, Germany). Each of the three sequential MRI examinations included pre-contrast T₁- and T₂-weighted fast spin echo (FSE), dynamic contrast enhanced (Figs. 1 and 2), and post-contrast SE T₁-weighted MRI imaging. Pre-contrast imaging included sagittal T₂-weighted images (TR = 4000–600 ms, TE = 100–120 ms, FOV = 30–40 cm, matrix = 256 × 192–256, slice thickness = 4 mm, gap = 1 mm, NEX = 2), axial T₂-weighted images (TR = 2500–3200 ms, TE = 100–120 ms, FOV = 30–40, matrix = 256 × 192–256, slice thickness = 7 mm, gap = 1 mm, NEX = 1–2) and axial T₁-weighted images (TR = 350–700, TE = 5–17, FOV = 30–40, matrix = 256 × 192–256, slice thickness = 7 mm, slice gap = 1 mm, NEX = 2–4) for optimal tumor localization and delineation (Figs. 1a and 2a). The post-contrast MRI used the same pulse sequence for the pre-contrast T₁-weighted SE image. Gadolinium MR contrast agent was given with a dose of 0.1 mmol/kg. For the DCE MRI (Figs. 1b and 2b), an intravenous bolus of 1 mmol/kg commercially available Gadolinium chelated MR contrast agent was given at a rate of no less than 5 ml/second using an MR-compatible power injector (Medrad Inc., Pittsburgh, PA).

DCE MRI

During the research period, two types of acquisition techniques, including the initial T₁-weighted single slice FSE imaging, and later a 3-D Gradient Recoiled Echo (GRE) volume imaging, were applied to optimize the balance between the quality of the DCE imaging data (temporal resolution) and the sampling volume (spatial resolution).

FSE DCE MRI acquisition technique—In the early part of the research only T₁-weighted FSE imaging was available to achieve adequate temporal resolution for quality DCE studies. However, this type of FSE acquisition technique limited the sampling volume and could only cover the majority of the tumor mass with a single thick slice profiled through the epicenter of the mass, where the most poorly-perfused hypoxic tumor region is likely located. The epicenter of the tumor mass was identified by axial and sagittal T₂-weighted FSE images, from which a single sagittal slice was determined for the T₁-weighted FSE DCE MRI study.

The T₁-weighted FSE DCE protocol included the following parameters: TR = 150 ms, TE = 18 ms, FOV = 30–40 cm, matrix = 128 × 192, and slice thickness = 1 cm. Immediately after the completion of more than five pre-contrast baseline acquisitions, the contrast agent was administered at a dose of 1 mmol/kg with an injection rate of 5–9 ml/second. DCE MRI was achieved with a temporal resolution of 3 seconds per acquisition and the acquisition continued for two minutes (40 images).

GRE Volume DCE MRI acquisition technique—With the advancement of the fast imaging techniques, the T₁-weighted 3D GRE acquisition technique was available during the later part of the research. This type of volume acquisition allowed coverage of the entire tumor volume with a reduced but adequate temporal resolution for the evaluation of the plateau SI of the DCE study.

The entire tumor volume, as determined by axial and sagittal T₂-weighted FSE images, was covered with the T₁-weighted 3D GRE volume acquisition. The imaging protocol included the following parameters: TR = 12.0–13.7 ms, TE = 4.2–5.0 ms, NEX = 1, flipangle = 30°, FOV = 30–40 cm, matrix = 160–192 × 256, partitions = 12, slab = 9.6 cm, slice thickness = 8 mm, and temporal resolution = 26–28 seconds. The total acquisition time was 158–168 seconds. A bolus injection of the contrast agent at a dose of 0.1 mmol/kg at a rate of 5 ml/second was initiated after completion of 3 pre-contrast 3D GRE baseline acquisitions.

Image Analysis

The original imaging data sets were transferred directly to the imaging laboratory for image analysis.

MRI volumetric analysis—The tumor region was outlined based on the hyperintense region on the T₂-weighted images in the sagittal plane by a radiologist and radiation oncologist. Tumor volume was calculated by pixel summation of all tumor areas outlined in each imaging slice, multiplied by slice thickness plus gap. *Initial tumor volume (V1)* was derived from the pre-treatment MRI study (MRI 1), and the residual tumor volumes (*V2* and *V3*) during treatment were derived, respectively, from the MRI 2 at 2–2.5 and MRI 3 at 4–5 weeks of radiation therapy.

DCE MRI analysis: SI, mean SI and SI percentiles—The regions of interest representing the tumor pixels on the T₂-weighted pre-contrast images were transferred to the DCE images for each MRI in each patient. Based on these regions of interest, signal intensity curves for each tumor pixel were generated from the DCE MRI datasets using an IDL (ITT Visual Information Solutions, Boulder, CO) based software developed in our laboratory. The SI of the plateau phase of the DCE curve was defined as SI. The SI of the DCE curve derived by the FSE acquisition technique was calculated from the least-square fit to the time/signal intensity curve (Figs. 1d and 2d), where SI changes were less than 20% for a time period of 10 seconds. Using this methodology, the time of the plateau phase of the SI curve usually ranged from 75–84 seconds of the FSE DCE curve. Because the DCE curve generated by the GRE volume acquisition technique had limited time points for the least square fit, the SI was determined at the time point of 75 seconds based upon the observations of the timing of plateau in the FSE DCE. The parameter *mSI* was generated by averaging the SI values of all pixels of the tumor region, and represents the mean perfusion of the entire tumor region.

An *SI-pixel distribution histogram* (Figs. 1c and 2c) of all tumor pixels' SIs was calculated and displayed, where the x-axis represents the SI values, and the y-axis represents the number (frequency) of pixels with same SI. The pixel SI histograms for each of the 3 sequential MRI studies of each of the 101 patients were analyzed to characterize the distribution of DCE of the pixels within the tumor. This allowed assessment the heterogeneity of the DCE and separation of pixel populations with low SI⁶, representing the low-perfusion regions of the tumor⁶ (Figs. 1c and 2c), which are likely to be therapy resistant and lead to treatment failure.

SI percentiles (SI%) were applied to characterize the degree (i.e. “how low”) and the quantity (i.e. “how many pixels”) of the low-DCE regions, i.e. the poorly perfused regions of the tumor. The SI percentiles (SI%) derived from the histogram, ranged from the 2.5th percentile (SI2.5%) through the 20th percentile (SI20%) in SI increments of 2.5%. For example, the SI5% of 2.41

in the patient shown in Figure 1c, represents the SI value, below which 5% of all pixels fall within this patient's heterogeneous tumor.

Assessment of Clinical Outcome Endpoints and Predictive Capacity

MRI parameters evaluated for the outcome prediction included initial 3D tumor volume V1, residual tumor volume V2 from MRI 2, and V3 from MRI 3, mean SI of the entire tumor volume (mSI), and SI percentiles (SI%), ranging from SI2.5% to SI20%, for each tumor and each imaging time point.

The clinical outcome endpoints included the control of the primary tumor (tumor control *vs.* recurrence) and the disease-free survival (alive *vs.* dead of cervical cancer), and were assessed by long-term post-therapy clinical follow-up. Control of the primary tumor was defined as no evidence of cancer in the pelvis by clinical (pelvic) examination and pap smear. Recurrence of the primary cancer was defined as either re-growth or persistence of the tumor in the cervix by clinical exam, biopsy and radiographic findings (if indicated). Post-therapy follow-up averaged 6.8 years with a range of 1.2 to 12.3 years. MRI-parameters were examined for their prediction power by correlation with the dichotomous outcome variables of primary tumor control and disease-free survival and by Kaplan Meier analysis of actuarial primary tumor control and disease-free survival rates. Differences among groups were estimated with the log-rank test.

Results

MRI parameters, including mean tumor SI (mSI), SI percentiles (SI%) and tumor volume (V), significantly predicted the long-term clinical outcome, including both control of the primary tumor and disease-free survival. Predictive MRI parameters were available as early as 2–2.5 weeks into the 8-week treatment course, at the time point of MRI 2. Table 1 provides a summary and comparison of the prediction provided by the individual MRI parameters at the three MRI study time points. The SI percentiles, ranging from SI5% to SI20%, provided overall the best prediction, with all except one p-value below 0.005 in discriminating primary tumor control, and all except one p-value below 0.03 for disease-free survival. The pixel histogram-based SI % parameters, which assessed the heterogeneity of DCE throughout the tumor, were superior to mSI (Table 1).

Analysis by Outcome End Point –Primary Tumor Control

Overall, low SI% values correlated with poor primary tumor control. The best single predictor for primary tumor control was SI5% at 2–2.5 weeks of therapy in MRI 2 ($p=0.0001$, Table 1). SI5% discriminated a 27% difference in primary tumor control. Patients with an SI5% of <2.05 in MRI 2 had an 8-year primary tumor control rate of only 73%, compared with 100% in those with SI5% values of ≥ 2.05 (Kaplan Meier analysis, $p=0.006$, log-rank test, Fig. 3). When analyzed by stage groups, SI5% of ≥ 2.05 *vs.* <2.05 in MRI2 showed large differences in primary tumor control rate within the stage I–II group (100% *vs.* 85%) and the stage III–IV group (100% *vs.* 58%), but these did not reach statistical significance.

Analysis by Outcome End Point –Disease-free Survival

The best single predictor for disease-free survival was the residual tumor volume V2 at 2–2.5 weeks of therapy in MRI 2 ($p=0.011$), followed by SI15% and SI20% at MRI 3 ($p=0.012$, Table 1). High V2 values correlated with poor disease-free survival. Patients with a V2 of ≥ 30 cm³ in MRI 2 had an 8-year disease-free survival rate of only 47%, compared with 79% for smaller V2 (Kaplan Meier Analysis, $p=0.001$, log-rank test, Fig. 4). When analyzed by stage groups, SI5% of ≥ 2.05 *vs.* <2.05 in MRI 2 showed non-statistically significant differences in disease-free survival within the stage I–II group (88% *vs.* 67%), and stage III–IV group (45% *vs.* 34%).

Analysis by MRI Study Time Point

When analyzed by MRI study time point with respect to the therapy course, MRI 2 provided the best prediction, based on the two parameters SI5% for primary tumor control (Fig. 3), and V2 for disease-free survival (Fig. 4). The prediction power of MRI 2 was followed by that of MRI 3 at 4–5 weeks of therapy. The parameters obtained by MRI 3, mSI and SI5% were significant but had less predictive power than the parameters in MRI 2 (Table 1). The pre-therapy MRI 1 provided the least prediction, and only one MR parameter, V1, the pre-therapy tumor volume, could predict disease-free-survival ($p=0.024$), but not control of the primary tumor (Table 1).

Analysis by Type of Parameter

Overall, the functional parameters obtained from the DCE MRI provided better prediction than the morphologic tumor volume parameters. Among the morphologic parameters of tumor volume, serial volume obtained during ongoing therapy, V2 and V3, was superior to the pre-therapy volume V1 in predicting primary tumor control and disease-free survival (Table 1). In contrast to the long-established paradigm of pre-therapy tumor volume as a powerful clinical prognostic factor for tumor control and survival, pre-therapy volume V1 showed prediction only for disease-free survival, and its prediction value was much lower than that of the residual volumes during the treatment, V2 and V3, or that of the functional SI% parameters obtained during the treatment (Table 1). When analyzed by stage subgroups, outcome differences based on V2 ($<30\text{ cm}^3$ vs. $\geq 30\text{ cm}^3$) were statistically significant for disease-free survival within the stage subgroup I–II (88% vs. 67%, $p=0.035$), but not within the stage subgroup III–IV (45% vs. 34%), or for the outcome endpoint primary tumor control (93% vs. 84%, and 82% vs. 57%, respectively).

Discussion

Tumor imaging during the early phase of a cytotoxic treatment course, within 2–4 weeks after initiation of treatment, as performed in our research, traditionally has not been implemented as routine procedure nor been incorporated into the management of cancer patients in the clinical setting. Such early timing, within weeks of the treatment start, may have much more powerful impact on the treatment choice and on ultimate outcome than the common concept of performing imaging after the completion of therapy for response assessment, that is currently in widely used in clinical oncology.

Based upon our overall results, the MRI parameters, SI5% and tumor volume, can predict, early during treatment, the ultimate long-term therapeutic outcome that, by standard evaluation methods, would not be evident until months or years after the completion of therapy. Our results show that this prediction could be made as early as 2 weeks into the 8-week treatment course (Table 1, Fig. 3).

Advanced cervical cancer is an excellent clinical model to study sequential functional (DCE) and morphological (volume) MRI parameters, and therefore is a disease well suited for the validation of an imaging-based predictive assay of long-term clinical outcome to an ongoing treatment. Cervical tumors can be readily imaged non-invasively by MRI providing multiplanar ability and superb anatomical soft tissue contrast for tumor delineation and volume measurement.^{20,21,22} Furthermore, the well-established functional relationship between tumor vascularity, hypoxia and radiation therapy outcome^{12,14,23,24} provides a unique tumor-biological basis to apply DCE MRI to study the functional tumor perfusion status during cytotoxic treatment.^{16,25} The stage distribution our study population is heterogeneous, but represents is typical for cohorts of patients treated with primary radiation therapy for cervical cancer.

Tumor Blood Supply and Long-term Therapeutic Outcome

Our results suggest that the poor outcome in those patients with DCE parameters indicative of low perfusion (Table 1, Fig. 3), is consistent with the long-held hypothesis that poor blood perfusion during treatment leads to radiation therapy failure.^{12,14,23,24,26} This is likely related to the presence of hypoxia in tumors with poor blood supply.²⁷ The clinical relevance of hypoxia in cervical cancer has been demonstrated by the correlation of needle oxymetry-based hypoxia with tumor recurrence.¹³ The adverse effect of low tumor perfusion has been suggested by the association of large intercapillary distances with tumor recurrence.¹⁴ Similarly, it is well known that the success of chemotherapy in cervical cancer is critically influenced by the effectiveness of vascular delivery of therapeutic agents into the interstitial space within the heterogeneous tumor.^{28,29} Both, adequate delivery of oxygen and chemotherapy agents depend on tumor blood supply and on the ability to extravasate the oxygen and chemotherapeutic agents through the vessel wall into the interstitial space and to the tumor cell.

Imaging Analysis of DCE MRI

DCE MRI has been established experimentally and clinically to characterize microvascular structure and function of tumors,^{3,5-7,30-32} to correlate with tumor oxygenation,²⁷ to assess treatment response of tumors and predict therapeutic outcome.^{4-6,8-10,16,33,34} Despite different imaging techniques, data analyses and tumor types, including our data, DCE MRI has shown considerable and consistent clinical relevance and the potential to further improve treatment strategies. With the limited and variable temporal resolutions, particularly during early part of our research, we had focused on analyzing the plateau SI of the DCE curve. We hypothesize, that among different imaging techniques, the plateau SI of the DCE curve reflects more consistently the effectiveness of the delivery of contrast agent, as well as oxygen and chemotherapy agents, to the interstitial space within the tumor, which critically influence the therapeutic effect and outcome.

Despite our variations in imaging techniques and MR scanners, our plateau-SI based results have consistently supported our hypothesis that DCE MRI parameters can provide critical information for the early prediction of long-term therapy outcome. With 101 patients our current study has the largest patient population with the longest follow-up time to date correlating both functional DCE and anatomical MRI parameters with therapy outcome in cervical cancer, and corroborates the findings of other smaller and shorter-term studies of DCE MRI in cervical cancer patients treated with cytotoxic therapy.^{6,17-19,35}

Our results are in overall agreement with our own prior pilot studies^{6,35} and with a study of 50 patients by Loncaster et al.¹⁹ despite it different DCE methodology. In Loncaster et al.'s study, the equilibrium method was used with the ROIs selected to include the maximal area of tumor involvement at the 12- and 6-o'clock positions of the cervix on a central sagittal tumor slice. DCE parameters were averaged over the ROI and included K_{ep} , Amplitude and maximal SIs, defined as maximal SI over baseline SI. High DCE shown by Amplitudes higher than the median Amplitude value, correlated with significantly improved disease-specific survival (~80% vs. ~60%, $p=0.024$; follow-up: 11-44 months, mean: 2 years). K_{ep} and SIs were not predictive of outcome. A study of 36 patients by Yamashita et al.¹⁸ evaluated pre-therapy DCE by the equilibrium method and by qualitative assessment. The ROI was defined as three 4-10-mm² ROIs that were representative of the tumor and DCE was analyzed by the multi-compartment model. Intense DCE pattern judged by qualitative assessment of enhancement and the transport parameter k correlated with tumor regression observed at the end of RT and tumor control at 1 year of follow-up. Despite these different imaging acquisition (equilibrium technique), tumor ROI determination (partially covering the tumor region), DCE modeling (2- or multi-compartment model) and lacking pixel-by-pixel heterogeneity analysis, these results of Loncaster and Yamashita et al.'s studies are in overall agreement with our results. This

literature comparison suggests that there is wide variability of DCE imaging and analysis methods in DCE in cervical cancer, and that our simpler and faster first-pass technique with heterogeneity analysis is at least as effective in predicting therapy outcome as the more complex and long acquisition times of the various equilibrium methods with mean DCE analyses.^{17–19} In addition, our study is the first to suggest that DCE and volume predicts outcome within FIGO stage subgroups, although the differences have not reached statistical insignificance, likely because of the smaller patient numbers within the stage subgroups.

In the only other study assessing DCE pattern *during* radiation therapy, Gong et al.¹⁷ showed in 7 patients that increase in mean and peak enhancement at 2 weeks of therapy correlated with tumor regression during therapy, but no follow-up outcome data is available. These short-term results are consistent with our long-term outcome correlation, and both suggest that the 2 weeks imaging time point may be superior. Further, our study is the first one to report a large patient population with a DCE MRI in the mid-phase of radiation therapy (MRI 3, 4–5 weeks after therapy start), and suggests that the DCE earlier in therapy (2–2.5 weeks after therapy start) has more predictive capacity for outcome. However, the result of the mid-radiation therapy MRI may be influenced by the confounding effects of beginning fibrosis, or by inflammatory changes caused by brachytherapy in 9 of the 101 patients, who had MRI 3 after their first brachytherapy procedure.

Improving Predictive Capacity by Analyzing Low-DCE Pixels and Residual Tumor Volume

While the above reports^{17–19} have largely employed mean enhancement, our study has focused on assessing the heterogeneity of DCE by developing our SI% parameters to quantitate poorly-perfused tumor pixels. Based upon our observations, the predictive power of the mSI, which averages the SI over the entire tumor, was not as strong as the SI% parameters (Table 1). The efficacy of mSI is expected to be limited, because the averaging of the SI over the entire tumor region may not adequately assess heterogeneity of tumor perfusion. Low-DCE components, which are more likely associated with therapy resistance, may be off-set by high-DCE components, reducing the overall discriminating power of the predictor. Heterogeneity within the same tumor (Figs. 1b and 2b) is a well known phenomenon.³⁶ Heterogeneous response to the ongoing treatment is not unexpected among different subregions within the same tumor³⁷ and can be critically influenced by regional variations in blood supply and hypoxia.^{26,28,38} The pixel SI histogram analysis developed in our study (Figs. 1c and 2c) has enabled us to assess heterogeneity and identify, separate, and quantify the poorly-enhanced low-DCE subregions. The superior prediction of tumor control and survival by our SI% compared to parameters that did not incorporate tumor heterogeneity, such as mSI or volume, suggests the efficacy of the SI% parameter in assessing relevant biological intra-tumoral heterogeneity that influences the tumor's responsiveness to cytotoxic treatment.

Our observation that the pre-therapy tumor volume was inferior to tumor volume regression obtained during therapy (Table 1) suggests that pre-therapy morphologic parameters are relatively less sensitive in predicting outcome. The residual tumor volumes, V2 and V3, after initiation of treatment, were superior to the pre-therapy volume measurements, likely because the subtle tumor volume change *during* therapy incorporates quantitative information on the responsiveness of the individual tumor to the early therapy effects.

Limitations of the research—There are several limitations of the current study. We recognize that our method of delineating the tumor ROI based upon the hyperintensity on the T₂-weighted images may not be ideal. Although the tumors with hyperintensity were readily visualized on the T₂-weighted images with the surrounding low SI background, including the air and normal cervix parenchyma, T₂-weighted images can potentially miss tumor regions with low SI, such as necrosis or hemorrhage, particularly if they are located at the periphery.

To achieve such long follow-up for clinical outcome validation of the imaging parameters, our study had to extend over long time periods to accrue sufficient patient numbers. Over this 12 year period, the image acquisition techniques for our research underwent progressive changes during significant advancements in MR imaging techniques. In the earlier period of our study, which benefits from the longest outcome follow-up, we could only implement a single-slice technique in order to provide sufficient temporal resolution for adequate DCE studies.

Although most of the hypoxic tumor mass was likely covered with our sampling technique of the center of the mass, it did not fully analyze the entire tumor volume due to the limited temporal and spatial resolution at the time of the imaging. In the later years of the study, when the recent rapid progress in fast imaging techniques provided much needed temporal and spatial resolution, the entire tumor volume could be included with the 3D GRE volume imaging protocol. With this technique, adequate DCE analysis of the plateau SI could still be achieved despite a sacrifice in temporal resolution.

With the variations of temporal resolution, our current research only focused on plateau SI but did not include the slope and washout phase of the DCE MRI parameters. Because compartmental analysis was not applied in the data analysis due to the limitation of our data, our semi-quantitative result is likely less accurate than that derived from the 2-compartmental analyses. Similarly, only one MR parameter, plateau SI, could be evaluated. Therefore multi-cluster vector analysis³⁹ was not applied in our data set to classify the pixel heterogeneity using various parts of the DCE curve. However, despite the limitations of variability in imaging techniques and platforms, we consistently find in the 101 patients throughout the study period that low DCE during cytotoxic therapy correlates clinically with long-term treatment failure. This finding suggests the clinical usefulness and validity of DCE MRI parameters in predicting therapy outcome in cervical cancer.

Conclusion

Our results show that MRI parameters quantifying heterogeneous tumor perfusion status and residual tumor volume can predict primary tumor control and survival well before completion of an ongoing cytotoxic therapy course. As early as 2–2.5 weeks into the treatment, early signs of ultimate treatment success or failure can be identified by DCE MRI, reflecting the heterogeneous delivery pattern of cytotoxic agents and oxygen, and by MRI-based residual tumor volume, presumably reflecting the bulk of therapy-resistant tumor. The imaging time point in early therapy was superior to the pre-therapy or later time points in therapy. Our current results require further validation in future studies.

Acknowledgments

Supported by NIH (contract grant number: RO1 CA 71906)

Abbreviations

DCE	Dynamic contrast-enhanced
FSE	Fast spin echo
FOV	field of view
GRE	Gradient recoiled echo
mSI	mean Signal intensity
OR	Odds ratio

NEX	number of excitations
SI	signal intensity
SI%	lowest percentile of signal intensity of poorly perfused tumor pixels
SI5%	lowest 5 th percentile of signal intensity of poorly perfused tumor pixels
TR	repetition time
TE	echo time
V	Tumor volume
V1	Initial tumor volume
V2	Residual tumor volume at MRI 2 (at 2–2.5 weeks)
V3	Residual tumor volume at MRI 3 (at 4–5 weeks)
3D	three-dimensional

References

1. Rose PG, Bundy BN, Watkins EB, et al. Concurrent Cisplatin-based radiotherapy and chemotherapy for locally advanced cervical cancer. *N Engl J Med* 1999;340:1144–1153. [PubMed: 10202165]
2. Eifel PJ. Problems with the clinical staging of carcinoma of the cervix. *Semin Radiat Oncol* 1994;4:1–8.
3. Taylor JS, Tofts PS, Port RE, et al. MR imaging of tumor microcirculation: promise for the new millennium. *J Magn Reson Imaging* 1999;10:903–907. [PubMed: 10581502]
4. Yuh WTC. An exciting and challenging role for the advanced contrast MR imaging. *J Magn Reson Imaging* 1999;10:221–222. [PubMed: 10508280]
5. Knopp MV, Giesel FL, Marcos H, von Tengg-Kobligk H, Choyke P. Dynamic contrast-enhanced magnetic resonance imaging in oncology. *Top Magn Reson Imaging* 2001;12:301–308. [PubMed: 11687716]
6. Mayr NA, Yuh WTC, Arnholt JC, et al. Pixel analysis of MR perfusion imaging in predicting radiation therapy outcome in cervical cancer. *J Magn Reson Imaging* 2000;12:1027–1033. [PubMed: 11105046]
7. Griebel J, Mayr NA, deVries A, et al. Assessment of tumor microcirculation - a new role of dynamic contrast MR imaging. *J Magn Reson Imaging* 1997;7:111–119. [PubMed: 9039600]
8. Hoskins PJ, Saunders MI, Goodchild K, Powell ME, Taylor NJ, Baddeley H. Dynamic contrast enhanced magnetic resonance scanning as a predictor of response to accelerated radiotherapy for advanced head and neck cancer. *Br J Radiol* 1999;72:1093–1098. [PubMed: 10700827]
9. George ML, Dzik-Jurasz AS, Padhani AR, et al. Non-invasive methods of assessing angiogenesis and their value in predicting response to treatment in colorectal cancer. *Br J Surg* 2001;88:1628–1636. [PubMed: 11736977]
10. Hawighorst H, Knopp MV, Debus J, Hoffman U, Grandy M. Pharmacokinetic MRI for assessment of malignant glioma response to stereotactic radiotherapy: initial results. *J Magnetic Resonance Imaging* 1998;8(4):783–788.
11. Lijowski M, Caruthers S, Hu G, et al. High sensitivity: high-resolution SPECT-CT/MR molecular imaging of angiogenesis in the Vx2 model. *Invest Radiol* 2009;44(1):1. [PubMed: 19060790]
12. Diesche S, Anderson PRS. Carcinoma of the cervix - anaemia, radiotherapy and hyperbaric oxygen. *Br J Radiol* 1983;56:251–255. [PubMed: 6831148]
13. Höckel M, Knoop C, Schlenger K, et al. Intratumoral pO₂ predicts survival in advanced cancer of the uterine cervix. *Radiother Oncol* 1993;26(1):45–50. [PubMed: 8438086]
14. Kolstad P. Intercapillary distance, oxygen tension and local recurrence in cervix cancer. *Scand J Clin Lab Invest* 1968;106(Suppl):145–157.

15. Eifel PJ, Morris M, Wharton JT, Oswald MJ. The influence of tumor size and morphology on the outcome of patients with FIGO stage IB squamous cell carcinoma of the uterine cervix. *Int J Radiat Oncol Biol Phys* 1994;29:9–16. [PubMed: 8175451]
16. Mayr NA, Hawighorst H, Yuh WTC, Essig M, Magnotta VA, Knopp MV. MR microcirculation in cervical cancer: correlations with histomorphological tumor markers and clinical outcome. *J Magn Reson Imaging* 1999;10:267–276. [PubMed: 10508286]
17. Gong QY, Brunt JN, Romaniuk CS, et al. Contrast enhanced dynamic MRI of cervical carcinoma during radiotherapy: early prediction of tumour regression rate. *Br J Radiol* 1999;72:1177–1184. [PubMed: 10703475]
18. Yamashita Y, Baba T, Baba Y, et al. Dynamic contrast-enhanced MR imaging of uterine cervical cancer: pharmacokinetic analysis with histopathologic correlation and its importance in predicting the outcome of radiation therapy. *Radiology* 2000;216:803–809. [PubMed: 10966715]
19. Loncaster JA, Carrington BM, Sykes JR, Jones AP, Todd SM, Cooper R. Prediction of radiotherapy outcome using dynamic contrast enhanced MRI of carcinoma of the cervix. *Int J Radiat Oncol Biol Phys* 2002;54:759–767. [PubMed: 12377328]
20. Hricak HLC, Sandles LG, et al. Invasive cervical carcinoma: comparison of MR imaging and surgical findings. *Radiology* 1988;166:623–631. [PubMed: 3340756]
21. Mayr NA, Yuh WTC, Taoka T, et al. Serial therapy-induced changes in tumor shape in cervical cancer and their impact on assessing tumor volume and treatment response. *AJR Am J Roentgenol* 2006;187:65–72. [PubMed: 16794157]
22. Mayr NA, Taoka T, Yuh WT, et al. Method and timing of tumor volume measurement for outcome prediction in cervical cancer using magnetic resonance imaging. *Int J Radiat Oncol Biol Phys* 2002;52(1):14–22. [PubMed: 11777618]
23. Höckel M, Schlenger K, Aral B, Mitze M, Schaffer U, Vaupel P. Association between tumor hypoxia and malignant progression in advanced cancer of the uterine cervix. *Cancer Res* 1996;56:4509–4515. [PubMed: 8813149]
24. Höckel MPV. Tumor hypoxia: definitions and current clinical, biologic, and molecular aspects. *J Natl Cancer Inst* 2001;93:266–276. [PubMed: 11181773]
25. Lyng H, Sundfor K, Trope C, Rofstad EK. Disease control of uterine cervical cancer: relationships to tumor oxygen tension, vascular density, and frequency of mitosis and apoptosis measured before treatment and during radiotherapy. *Clin Cancer Res* 2000;6:1104–1112. [PubMed: 10741740]
26. Gray LH, Conger AD, Ebert M, Hornsey S, Scott OC. The concentration of oxygen dissolved in tissues at the time of irradiation as a factor in radiotherapy. *Br J Radiol* 1953;26:638–648. [PubMed: 13106296]
27. Cooper RA, Carrington BM, Loncaster JA, et al. Tumour oxygenation levels correlate with dynamic contrast-enhanced magnetic resonance imaging parameters in carcinoma of the cervix. *Radiation Oncol* 2000;57:53–59. [PubMed: 11033189]
28. Link KH, Leder G, Pillasch J, et al. In vitro concentration response studies and in vitro phase II tests as the experimental basis for regional chemotherapeutic protocols. *Semin Surg Oncol* 1998;14:189–201. [PubMed: 9548601]
29. Simpson-Herren L, Noker PE, Wagoner SD. Variability of tumor response to chemotherapy. II. Contribution of tumor heterogeneity. *Cancer Chemother Pharmacol* 1988;22:131–136. [PubMed: 3409443]
30. Brix G, Schreiber W, Hoffmann U, Guckel F, Hawighorst H, Knopp MV. Methodological approaches to quantitative evaluation of microcirculation in tissues with dynamic magnetic resonance tomography [Review]. *Radiologe* 1997;37(6):470–480. [PubMed: 9340677]
31. Mayr NA, Yuh WT, Zheng J, et al. Prediction of tumor control in patients with cervical cancer: analysis of combined volume and dynamic enhancement pattern by MR imaging. *Am J Roentgenol* 1998;170(1):177–182. [PubMed: 9423627]
32. Tofts PS, Brix G, Buckley DL, et al. Estimating kinetic parameters from dynamic contrast-enhanced T1-weighted MRI of a diffusible tracer: standardized quantities and symbols. *J Magn Reson* 1999;10:223–232.
33. Knopp M, Weiss E, Sinn HP, et al. Pathophysiologic basis of contrast enhancement in breast tumors. *J Magn Reson Imaging* 1999;10:267–285. [PubMed: 10508286]

34. Wenz F, Rempp K, Hess T, et al. Effect of radiation on blood volume in low-grade astrocytomas and normal brain tissue: quantification with dynamic susceptibility contrast MR imaging. *AJR Am J Roentgenol* 1996;166:187–193. [PubMed: 8571873]
35. Mayr NA, Yuh WTC, Magnotta VA, et al. Tumor perfusion studies using fast magnetic resonance imaging technique in advanced cervical cancer - a new non-invasive predictive assay. *Int J Radiat Oncol Biol Phys* 1996;36:623–633. [PubMed: 8948347]
36. Lyng H, Vorren AO, Sundfor K, et al. Intra- and intertumor heterogeneity in blood perfusion of human cervical cancer before treatment and after radiotherapy. *Int J Cancer* 2001;96:182–190. [PubMed: 11410887]
37. Suit H, Skates S, Taghian A, Okunieff P, Efid JT. Clinical implications of heterogeneity of tumor response to radiation therapy. *Radiotherapy and Oncology: Journal of the European Society for Therapeutic Radiology and Oncology* 1992;25(4):251–260. [PubMed: 1480770]
38. Overgaard J, Horsman MR. Modification of hypoxia-induced radio-resistance in tumors by the use of oxygen and sensitizers. *Semin Radiat Oncol* 1996;6:10–21. [PubMed: 10717158]
39. Schlossbauer T, Leinsinger G, Wismuller A, et al. Classification of small contrast enhancing breast lesions in dynamic magnetic resonance imaging using a combination of morphological criteria and dynamic analysis based on unsupervised vector-quantization. *Invest Radiol* 2008;43(1):56–64. [PubMed: 18097278]

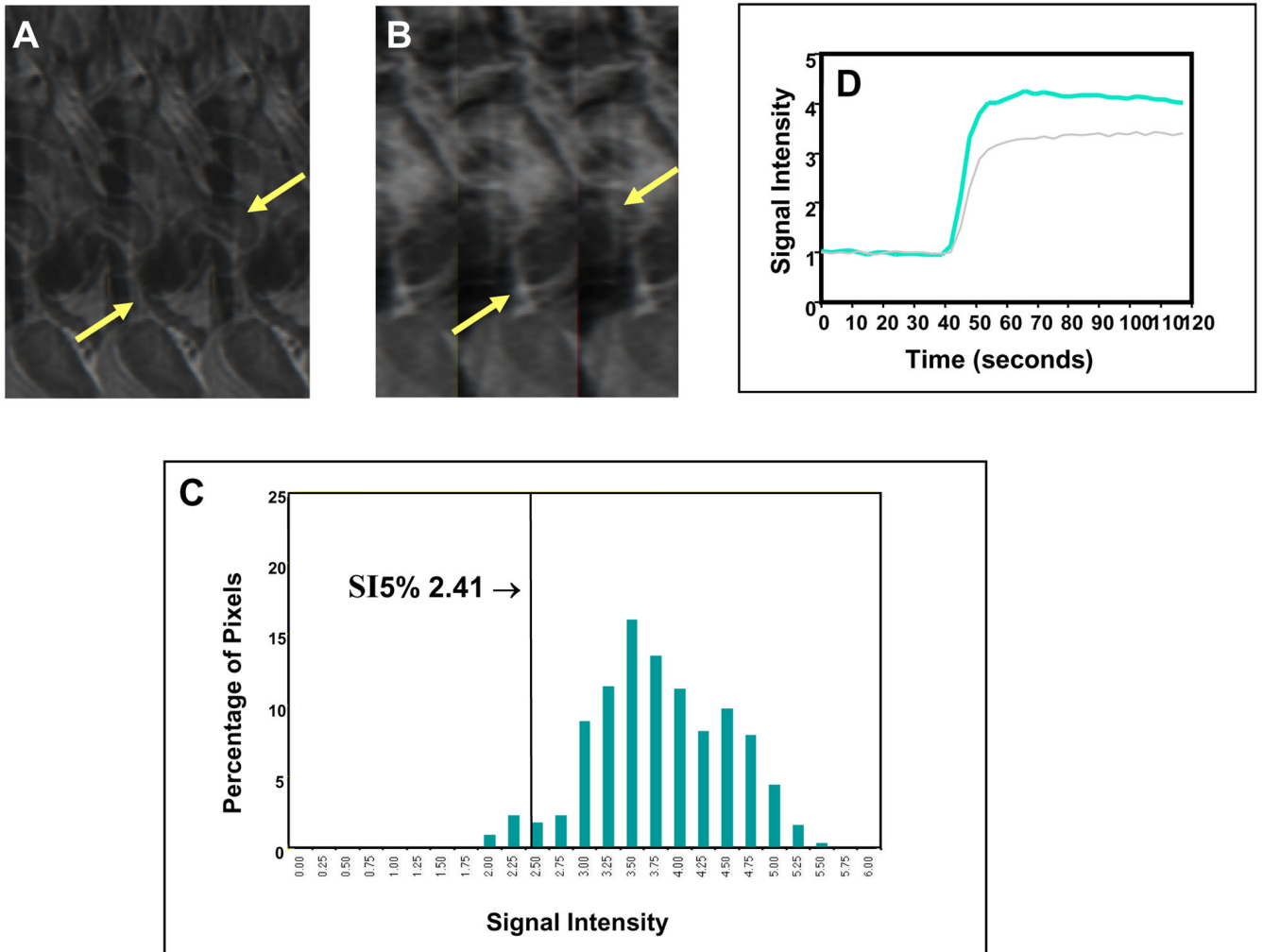


Fig. 1. Favorable clinical outcome with high perfusion status early during treatment in a large tumor

Pre-contrast sagittal T₂-weighted image (A) shows a large cervical cancer (arrows) indicating poor prognosis as judged by FIGO criteria. Corresponding DCE MRI at the plateau phase of the DCE imaging (B) shows the large tumor (arrows) with intense and heterogeneous dynamic contrast enhancement, indicating high tumor perfusion during the early part (2 weeks) of the 8-week treatment course. Tumor SI-pixel histogram (C) of the tumor is generated with the SI of the entire tumor pixels by plotting the SI of each tumor pixel along the x-axis and the number of pixels with same SI (frequency) along the y-axis. From this tumor SI-histogram, tumor size (area under the DCE curve) can be calculated. The quantity and degree of low DCE sub-population was quantified by computing SI percentiles. In this case, the 5th percentile (SI5%) (arrow, C) was 2.41, indicating that 5% of the pixels within the heterogeneous tumor fall below an SI of 2.41. This patient had excellent treatment outcome and survived for the past 8 years. Signal intensity-time DCE curves (D) again show abrupt and intense contrast enhancement of the tumor, indicating high tumor perfusion in both MRI 1 (gray-colored curve) and MRI 2 (blue-colored curve), and predicting excellent response and long-term outcome to treatment.

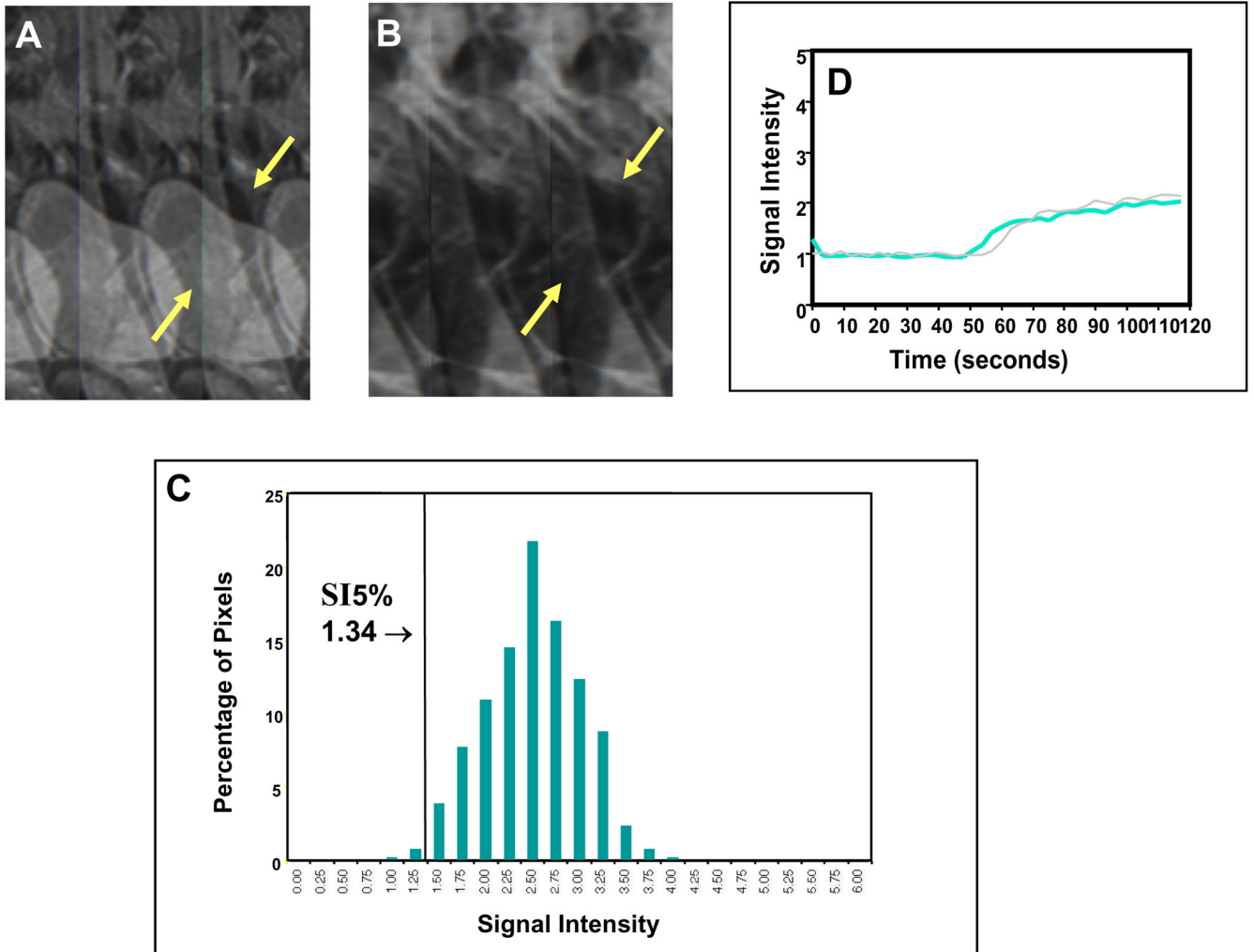


Fig. 2. Poor clinical outcome with low perfusion status early during treatment for a small tumor Pre-contrast sagittal T₂-weighted image (**A**) showed a much smaller cervical cancer (arrows), as compared to Fig. 1, indicating a more favorable prognosis as judged by FIGO criteria. Corresponding DCE MRI at the plateau phase of the DCE imaging (**B**) showed the small tumor (arrows) with poor contrast enhancement indicating low tumor perfusion during early part (2 weeks) of the treatment course (8 weeks). From the tumor SI-pixel histogram (**C**), the low-DCE sub-population was characterized by 5th percentile of SI (SI5%). SI5% was much lower (1.34) than that of Fig. 1 (2.41). This patient had a primary tumor recurrence at 2 months after completion of therapy, and died 6 months after completion of therapy. Signal intensity-time DCE curves (**D**) again show sluggish and low contrast enhancement of the tumor mass indicating low tumor perfusion and poor response to treatment. In contrast to Figure 1, tumor perfusion remains low even 2–3 weeks after initiation of therapy (blue-colored curve) and is similar to that of the pretreatment (gray-colored curve).

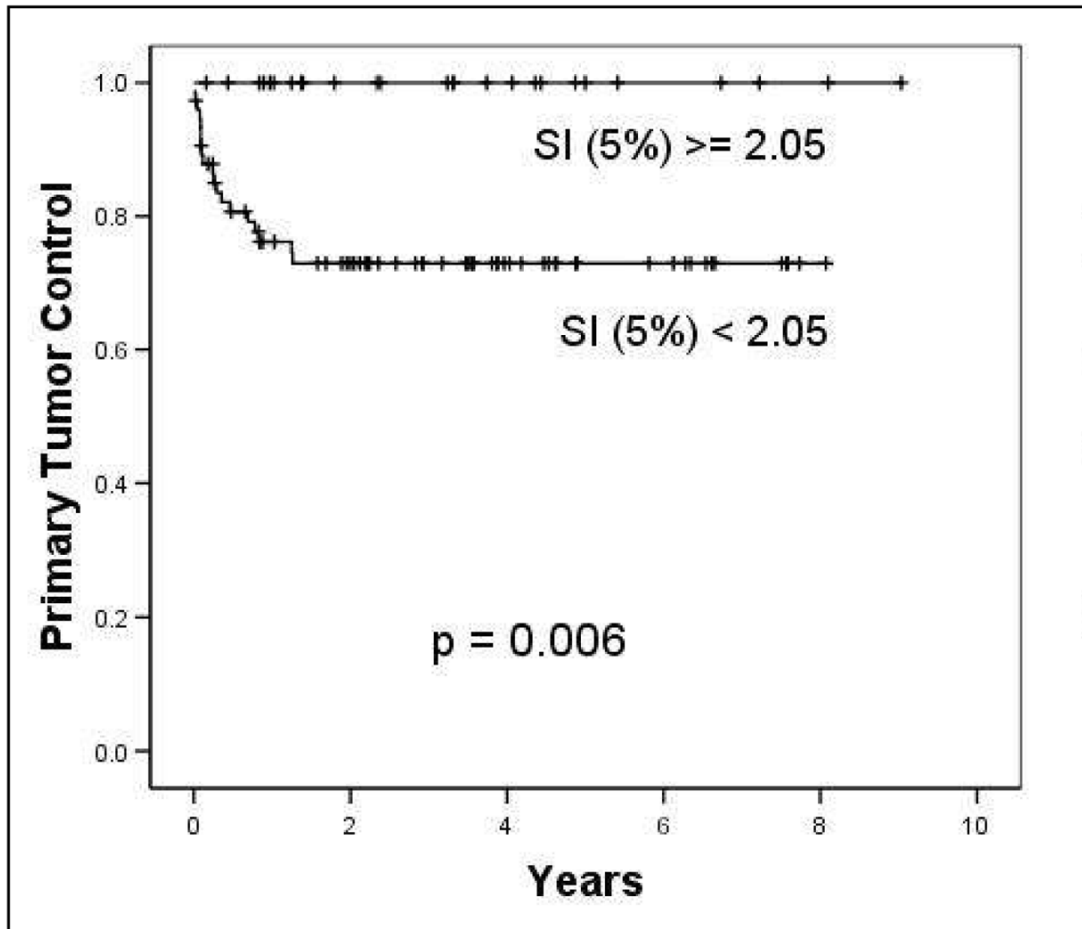


Fig. 3. Primary tumor control and disease-free survival based on SI5% at MRI 2
Kaplan Meier Life Table analysis shows a significantly better 8-year primary tumor control rate for patients with $SI5\% \geq 2.05$, compared to those patients with lower SI5% indicative of low DCE (100% vs. 73%, $p = 0.006$, Log rank test).

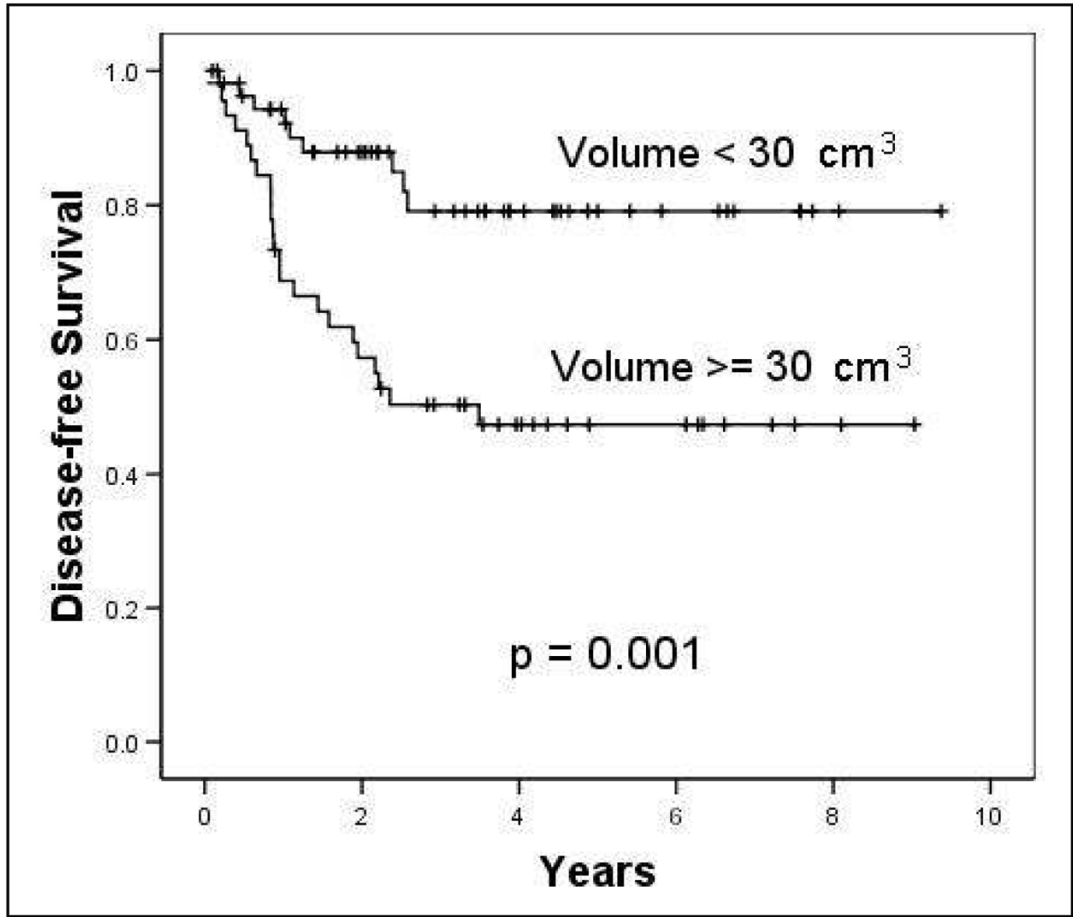


Fig. 4. Primary tumor control and disease-free survival based on tumor volume V2 at MRI 2
Kaplan Meier Life table analysis shows a significantly better 8-year disease-free survival for patients with a V2 <30 cm³, compared to those patients with higher V2 (79 vs. 47%, p= 0.001, Log rank test).

MRI prediction value for primary tumor control and disease-free survival before and during therapy

Table 1

MRI Parameters	Control of Primary Tumor	MRI 1	MRI 2	MRI 3	MRI 1	MRI 2	MRI 3
Volume	NS	0.012	0.025	0.024	0.011	NS	NS
Mean SI	NS	0.015	0.040	NS	NS	NS	0.029
SI (2.5%)	NS	0.00030	0.00116	NS	NS	NS	0.032
SI (5.0%)	NS	0.00010	0.00176	NS	NS	NS	0.024
SI (10%)	NS	0.00124	0.00331	NS	NS	NS	0.017
SI (15%)	NS	0.00187	0.00473	NS	NS	NS	0.012
SI (20%)	NS	0.00402	0.00786	NS	NS	NS	0.012

Note: Numerical values are p-values from Student t-test; NS = not significant ($p > 0.05$). MRI 1, MRI 2, and MRI 3 were obtained before treatment, at 2–2.5 weeks, and 4–5 weeks, respectively, into the 8 weeks treatment course; SI% = percentile of signal intensity, including 2.5th, 5th, 10th, 15th, and 20th percentiles of SI, to quantify the low-DCE pixel sub-populations within the tumor.